

## Supplementary information

### **MXene–TMD Heterostructure Photodetector: Engineering Ti<sub>3</sub>C<sub>2</sub>/SnS<sub>2</sub> Interface for High-Speed Visible Light Detection**

Chayan Das<sup>a</sup>, Suresh Kumar<sup>a</sup>, Jeny Gosai<sup>c</sup>, Mubashir Mushtaq Ganaie<sup>a</sup>, Anjali Sharma<sup>d,e</sup>, Mahesh Kumar<sup>b</sup>, Ankur Solanki<sup>c</sup>, Arup K. Rath<sup>d,e</sup>, Satyajit Sahu<sup>a\*</sup>

<sup>a</sup>Department of Physics, Indian Institute of Technology Jodhpur, Jodhpur 342037, India

<sup>b</sup>Department of Electrical Engineering, Indian Institute of Technology Jodhpur, Jodhpur 342037, India

<sup>c</sup>Department of Physics, School of Energy Technology, Pandit Deendayal Energy University, Gandhinagar 382426, India

<sup>d</sup>CSIR-National Chemical Laboratory, Dr. Homi Bhabha Road, Pune 411008, India

<sup>e</sup>Academy of Scientific and Innovative Research, Ghaziabad, 201002, India

email: [satyajit@iiitj.ac.in](mailto:satyajit@iiitj.ac.in)

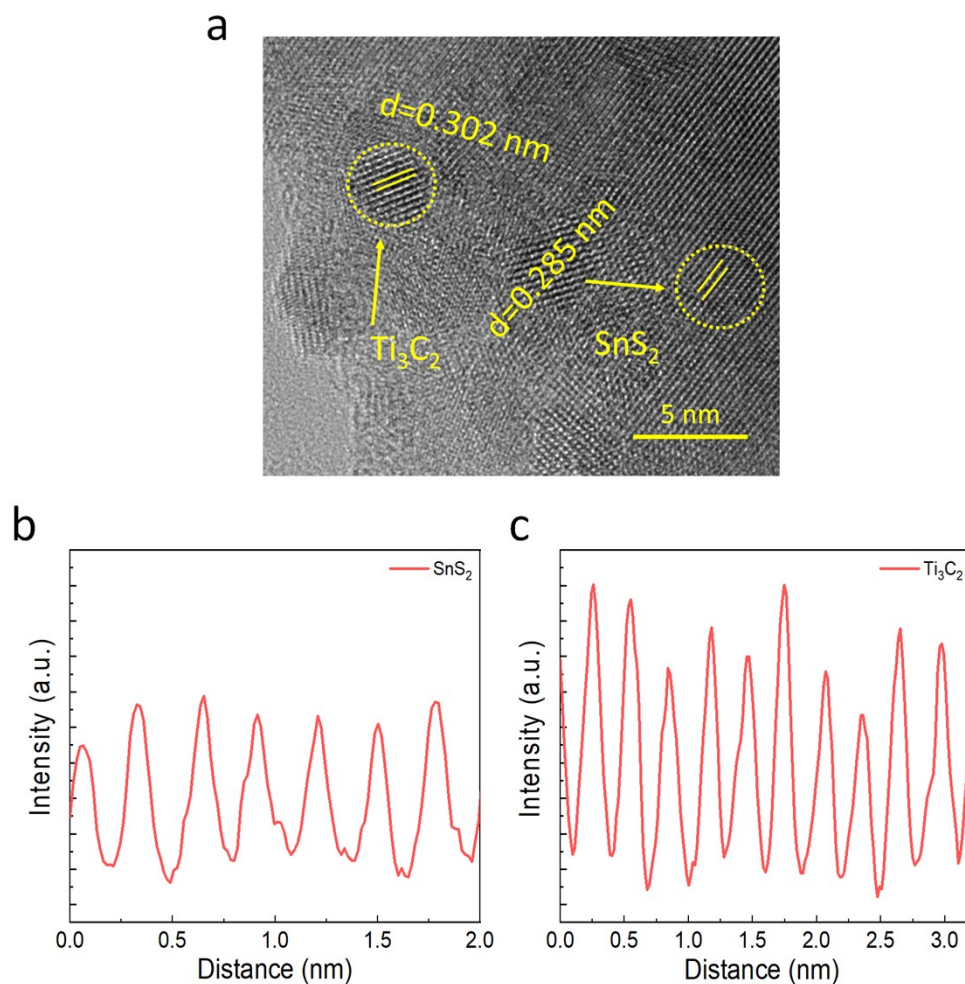


**Figure S1:** (a) HRTEM image of  $\text{Ti}_3\text{C}_2/\text{SnS}_2$  heterostructure with distance profile scans at specific regions of (b)  $\text{SnS}_2$  and (c)  $\text{Ti}_3\text{C}_2$ .

The HRTEM image of  $\text{Ti}_3\text{C}_2/\text{SnS}_2$  heterostructure is shown in **Figure S1 a**. The distance profile scan of  $\text{SnS}_2$  is shown in **Figure S1 b**, and the average interplanar distance was found to be 0.285 nm. The distance profile scan of  $\text{Ti}_3\text{C}_2$  is shown in **Figure S1 c**, and the average interplanar distance was found to be 0.302 nm.

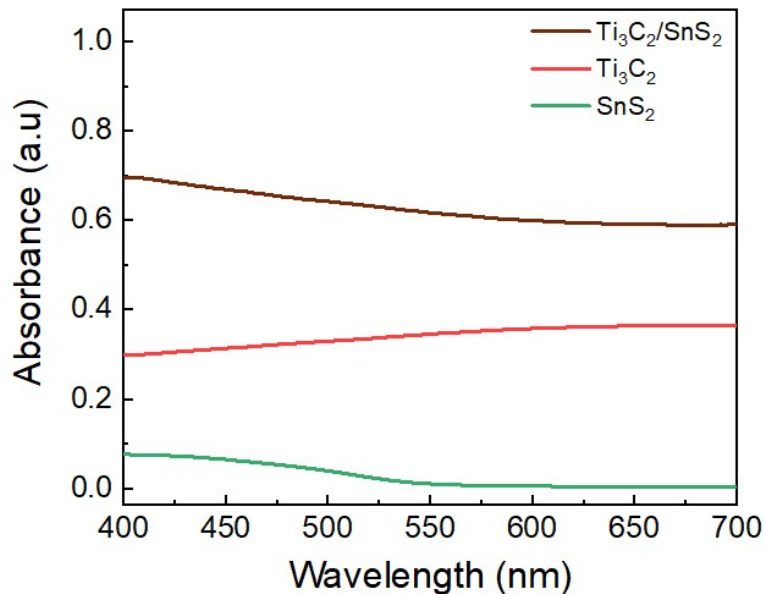


**Figure S2:** Representation of absorbance of  $\text{SnS}_2$ ,  $\text{Ti}_3\text{C}_2$ , and  $\text{Ti}_3\text{C}_2/\text{SnS}_2$  with respect to wavelength.

The absorbance of  $\text{SnS}_2$ ,  $\text{Ti}_3\text{C}_2$ , and  $\text{Ti}_3\text{C}_2/\text{SnS}_2$  with respect to wavelength is shown in **Figure S2a**. It shows an improved absorption of  $\text{Ti}_3\text{C}_2/\text{SnS}_2$  compared to both individual components. For our sample (solid sample) we used diffused reflectance in the integrating sphere embedded in the system and used the Kubelka-Munk transformation function to calculate the absorbance.

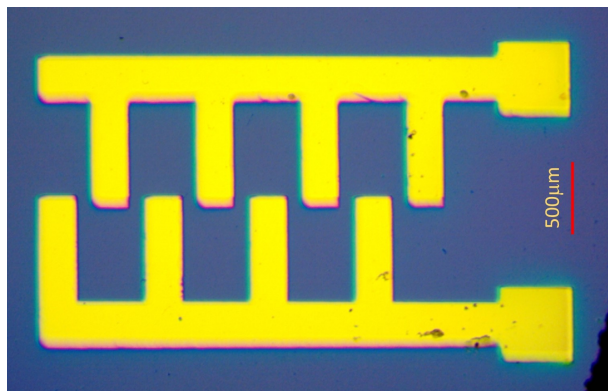


**Figure S3:** Image of one individual device (cell) with scale bar of 500  $\mu\text{m}$ .

The device image is shown in **Figure S3**. The image of one individual device (cell) is shown in **Figure S3a**.

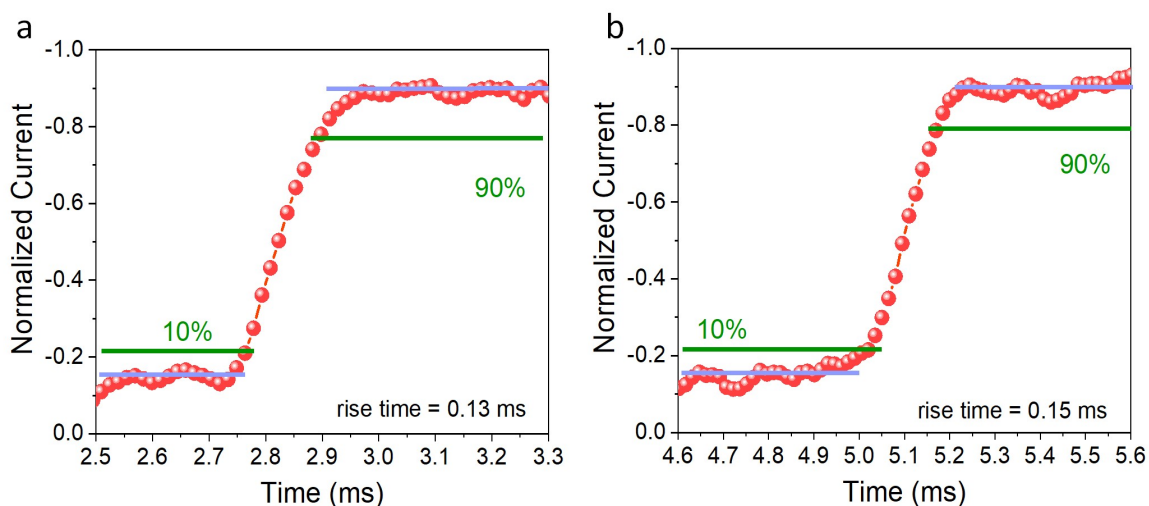


**Figure S4:** Rise time calculation of  $\text{Ti}_3\text{C}_2/\text{SnS}_2$ -based device (a) set 1, (b) set 2, with bias voltage of -5V and under light of 455 nm wavelength and intensity of  $100 \mu\text{W}/\text{cm}^2$ .

The time necessary to change the photocurrent from 10% to 90% was used to compute the response time. We repeated the experiment of determining the  $\text{Ti}_3\text{C}_2/\text{SnS}_2$ -based device. It exhibited a rise

time of 0.13 (Figure S4 a) and 0.15 ms (Figure S4 b). And the rise time shown in (Figure 8 d) is 0.17 ms. The average rise time  $(0.13 + 0.15 + 0.17) \text{ ms}/3 = 0.15 \text{ ms}$ .

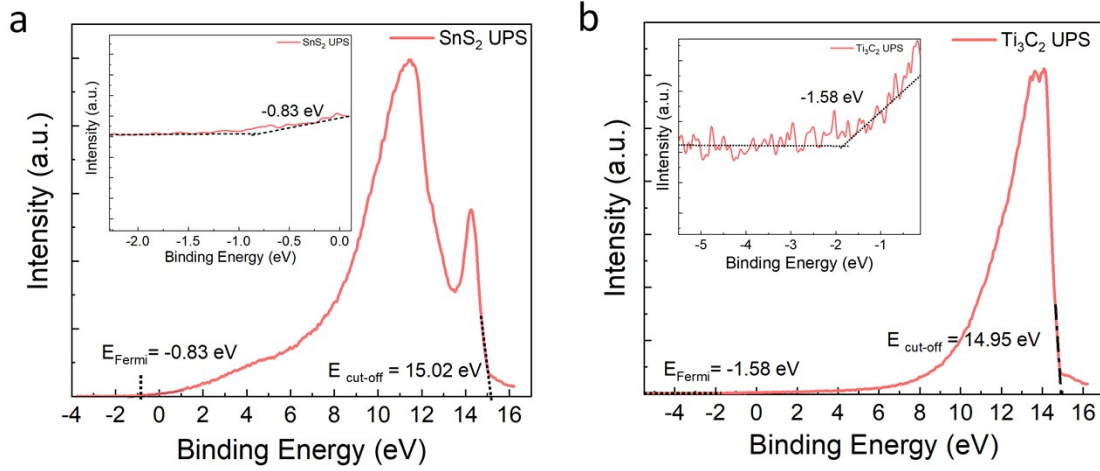


**Figure S5:** Ultraviolet photoelectron spectroscopy (UPS) spectrum plot of (a) SnS<sub>2</sub> and (b) Ti<sub>3</sub>C<sub>2</sub> with respect to energy.

The ultraviolet photoelectron spectroscopy (UPS) measurement was performed using a He-I $\alpha$  light source with an energy of 21.22 eV. The UPS plot of SnS<sub>2</sub> is shown in **Figure S5 a**. The work function (WF) was calculated using the formula  $WF = 21.22 - E_{\text{cut-off}} - E_{\text{Fermi}} = 5.37 \text{ eV}$ . The WF of Ti<sub>3</sub>C<sub>2</sub> was also calculated to be 4.70 eV from the UPS plot of **Figure S5 b**.

We fabricated four Ti<sub>3</sub>C<sub>2</sub>/SnS<sub>2</sub> devices, i.e., D1, D2, D3, and D4, excluding our studied device, on which pristine SnS<sub>2</sub> also showed interconnectedness across the channel, in a single wafer. Their photo and dark current levels, and photo to dark current ratio were added in Table S1.

**Table S1:** Obtained photo and dark current levels, and photo to dark current ratio of another four Ti<sub>3</sub>C<sub>2</sub>/SnS<sub>2</sub> based devices with a bias voltage of -5V, and wavelength of 455 nm along with an intensity of 7.5 mW/cm<sup>2</sup>.

Device	$I_{ph}$ (A)	$I_{dark}$ (A)	$I_{ph}/I_{dark}$
D1	$1.31 \times 10^{-5}$	$1.44 \times 10^{-7}$	153
D2	$4.32 \times 10^{-6}$	$1.09 \times 10^{-7}$	39
D3	$4.83 \times 10^{-6}$	$1.08 \times 10^{-7}$	33

D4	$3.21 \times 10^{-6}$	$1.16 \times 10^{-7}$	28
----	-----------------------	-----------------------	----

The current levels of  $\text{Ti}_3\text{C}_2/\text{SnS}_2$  device in presence and absence of light are denoted as  $I_{ph}$  and  $I_{dark}$  with a wavelength 405 nm of and an intensity of  $7.50 \text{ mW/cm}^2$ . The max photo-to-dark current ratio  $I_{ph}/I_{dark}$  for all these devices are calculated. As their ratio is less than our reported device, we did not proceed with the other characterizations, considering it a low-performance device.

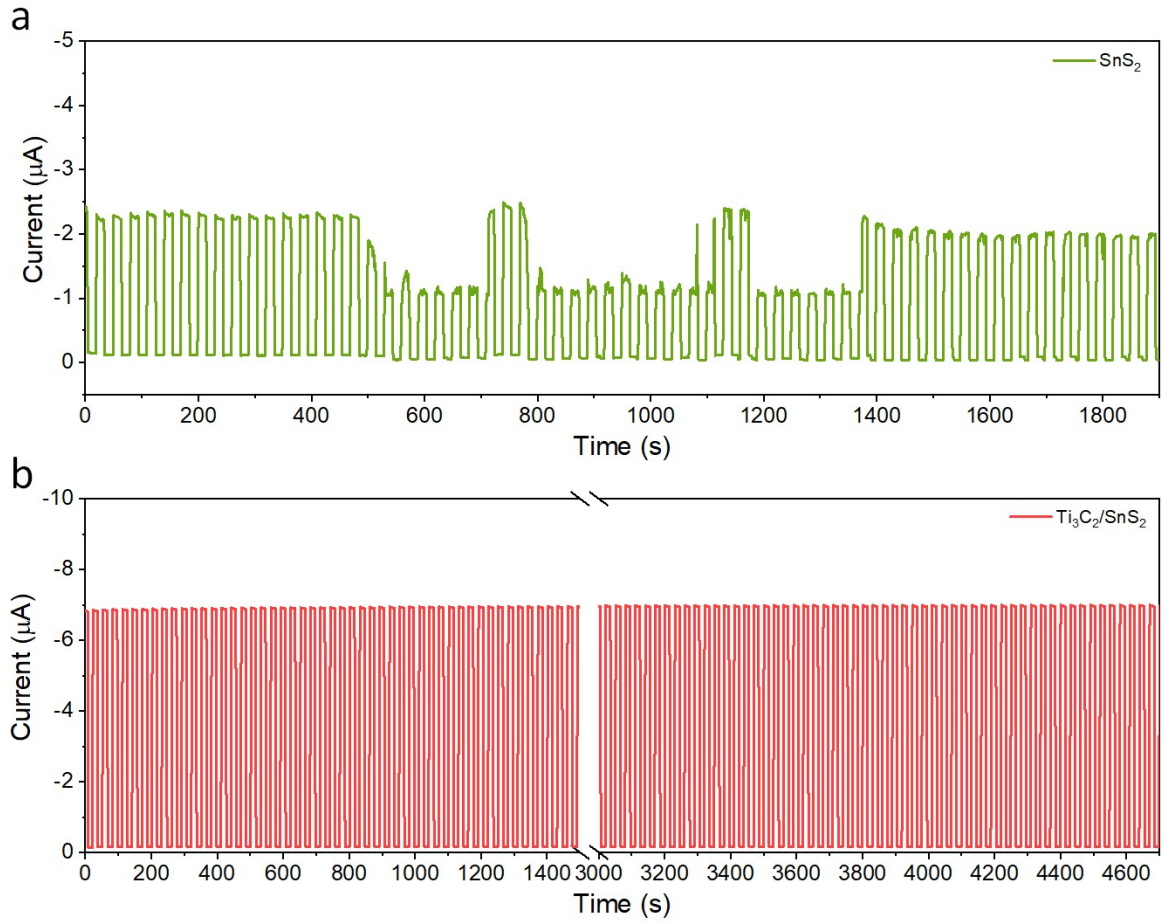


**Figure S6:** (a) Cycling performance of pristine  $\text{SnS}_2$ -based device for 1900 s under continuous illumination (455 nm,  $100 \mu\text{W cm}^{-2}$ , pulse width 15 s).

(b) Cycling performance of  $\text{Ti}_3\text{C}_2/\text{SnS}_2$ -based device after one-month ambient storage for 4700 s under the same conditions.

The same cycle test was performed with only the  $\text{SnS}_2$ -based device after one month by applying sequential pulses with a pulse width of 15s. The device's response clearly shows its degradation in the ambient. The test lasted for 1900 s (**Figure S6a**), indicating poor stability under ambient conditions. One of the possible reasons is electrochemical reactions in the presence of light, oxygen, and humidity <sup>17</sup>. It affects the photoinduced electrons/holes at the interface of materials by redox reaction. In presence of oxygen,  $\text{NO}_2$  and, toxic gases the materials create different kind of oxide nitride and salts which permanent damage in device performance <sup>18</sup>. But on the other hand, the  $\text{Ti}_3\text{C}_2/\text{SnS}_2$ -based device showed its excellent stability after one month in ambient (**Figure S6b**), which shows its potential against absorbents like moisture, oxygen, etc.

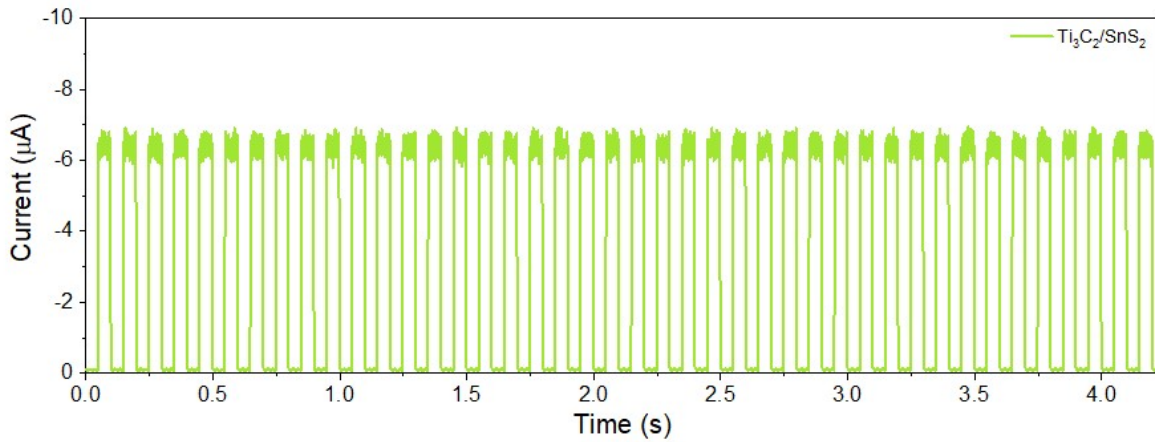


**Figure S7:** Cycle test of the  $\text{Ti}_3\text{C}_2/\text{SnS}_2$  photodetector performed after five months in ambient conditions using 100 ms light pulses at 455 nm and  $100 \mu\text{W cm}^{-2}$ , with a sampling interval of 0.56 ms per point.

The  $\text{Ti}_3\text{C}_2/\text{SnS}_2$  device shows clear and reproducible on/off transitions within the 4.5 s test duration, corresponding to ~45 cycles. The extracted rise and decay times ( $\sim 0.15$  ms and  $\sim 0.17$  ms) are consistent with Figure 8, confirming that the device remains fully functional under rapid optical modulation and validating its high-speed photoresponse capability.

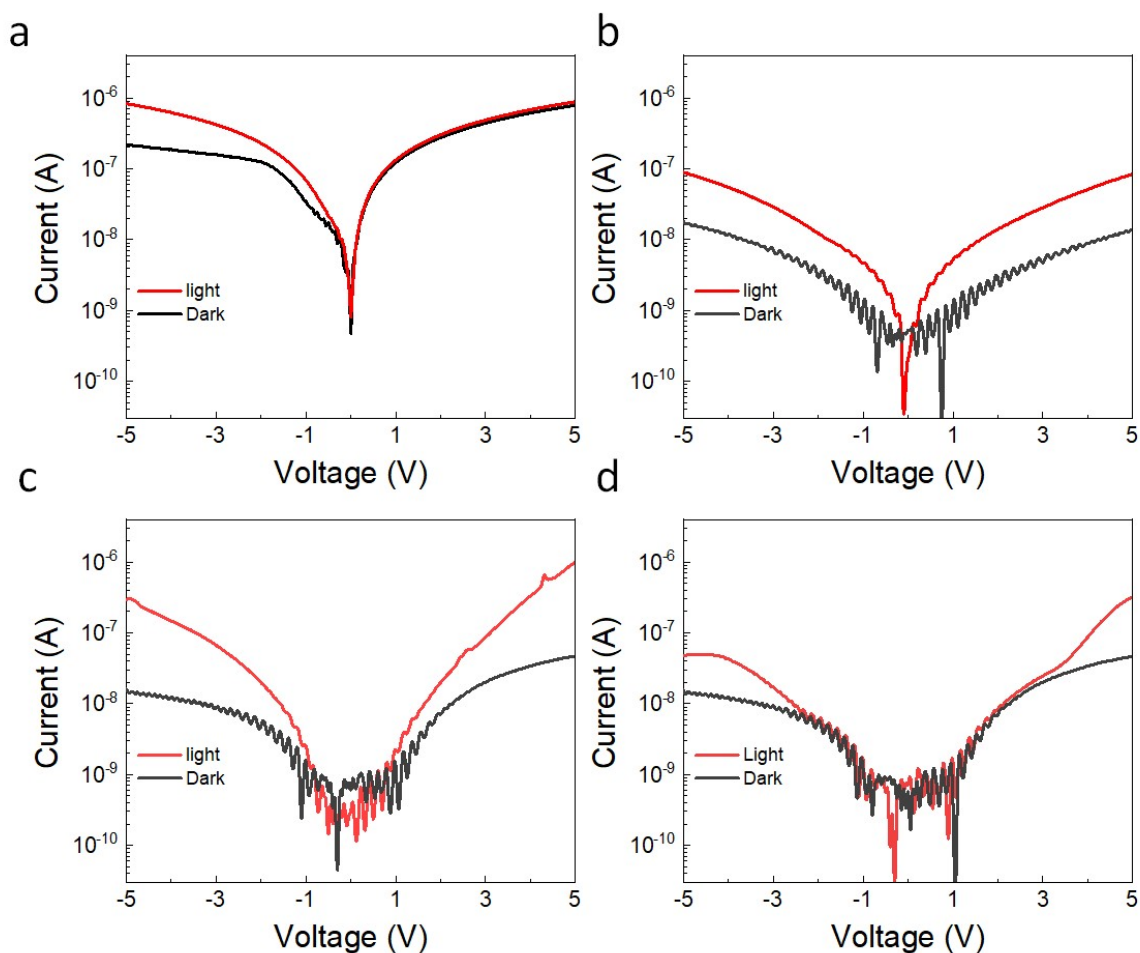


**Figure S8:** The I-V characteristic of  $\text{Ti}_3\text{C}_2\text{-SnS}_2$ -devices drop casted with different concentrations (a) 2 mg/L (b) 1 mg/L, (c) 0.5 mg/L, (d) 0.1 mg/L of  $\text{Ti}_3\text{C}_2$  with a bias voltage of -5V, and wavelength of 455 nm along with an intensity of  $7.5 \text{ mW/cm}^2$ .

The photo-to-dark current ratios were found to be 3.8, 5.5, 15.2, and 3.2 for 2, 1, 0.5, and 0.1  $\text{mg L}^{-1}$ , respectively. The optimized concentration of 0.5  $\text{mg L}^{-1}$  provided the highest performance and was used in the reported device. These results demonstrate the influence of  $\text{Ti}_3\text{C}_2$  loading on interfacial charge transport and overall photodetection efficiency.